

NASA Contractor Report 187510

117-51
8411
P36

(NASA-CR-187510) POWER OPTIMAL SINGLE-AXIS
ARTICULATING STRATEGIES (Analytical
Mechanics Associates) 36 p CSCL 20K

N91-21581

Unclas
G3/39 0008411

131

POWER OPTIMAL SINGLE-AXIS ARTICULATING STRATEGIES

Renjith R. Kumar
Michael L. Heck

ANALYTICAL MECHANICS ASSOCIATES, INC.
Hampton, Virginia

Contract NAS1-18935
February 1991



National Aeronautics and
Space Administration

Langley Research Center
Hampton, Virginia 23665

Table of Contents

Introduction	1
Problem Formulation (Beta-tracking)	2
Mathematical Model	2
Solution Procedures	5
Numerical Results (No Shadowing Considerations)	6
LVLH Station Core Attitude	6
Non-LVLH Station Attitude	8
Numerical Results with Intra-array Shadowing	8
A Comparison to Optimal Alpha-only Tracking	10
Conclusions	12
Optimal Beta-tracking Strategy	12
Optimal Alpha-tracking Strategy	12

1. INTRODUCTION

The baseline assembly complete configuration of Space Station Freedom is comprised of an inner core and outer articulating parts as shown in Figure 1. The attitude of the inner core, comprising the module cluster, center truss, etc., must be maintained close to a local vertical local horizontal (LVLH) attitude using active control devices such as Control Moment Gyros (CMGs) and/or Reaction Control System (RCS) thrusters. This attitude control is necessary to accommodate microgravity and pointing requirements for user payloads located in the inner core. The power required for the Space Station is provided by photovoltaic (PV) arrays located on the port and starboard articulating structures.

The PV arrays have to continuously track the sun to provide the required electrical power. Due to the motion of the Space Station along its orbit, variations in orbital geometry with respect to the sun, and the core attitude fluctuations with respect to the LVLH orientation due to disturbing external torques, the orientation of the PV arrays must be constantly adjusted with respect to the inner core to track the sun. The physical rotary joints which perform this function are called the Solar Alpha Rotary Joints (alpha joints) and the Solar Beta Rotary Joints (beta joints). The alpha joints provide a relative rotational motion between the inner core and the outboard truss. The beta joints perform the PV array orientation adjustment with respect to the articulating port and starboard truss. Assuming the station is at an LVLH attitude, the alpha joint rotation rate would be the orbital rate. The beta joint rotation varies slowly over an orbit and the yearly variation follows the solar beta history. The definition of the *solar beta* angle is shown in Figure 2a.

In this report, the authors investigate the power loss resulting from the elimination of one of the articulating joints. The objective of this study is to maximize available power with only one rotary joint.

The motivation to eliminate the alpha joint is to reduce the cost of the station. The outboard truss and beta joint axis is aligned to minimize drag on the PV arrays and this corresponds to a feathered array orientation for an LVLH core attitude as shown in Figure 1. Optimal beta gimbal strategies are investigated. The power study is performed for LVLH and non-LVLH station attitudes. Intra-array shadowing, shadowing thresholds, and power loss from shadowing are also addressed. Alternatively, power loss due to elimination of

beta joints, with alpha gimbal reinstated is examined for comparison of available power.

2. PROBLEM FORMULATION (BETA-TRACKING)

Two optimal beta joint control problems are addressed in this paper and can be may be stated as follows:

- 1) Evaluate the optimal *variable* beta angle history for the Space Station over a given orbit that maximizes the integral of the dot product of the unit vector from the spacecraft to the sun and the unit vector normal to the active side of the PV array over orbital daylight. The attitude of the core of the station is assumed to be LVLH. The dot product quantity is named **direct sunlight factor** in this study. The integral of the direct sunlight factor over orbital daylight provides a total measure of useful solar power over the entire orbit.
- 2) Evaluate the optimal *constant* beta angle which has to be maintained over a given orbit, for the Space Station, that would maximize the same performance index as above.

It is obvious that the solution to problem 1 (p1) would yield an equal or better performance index than the solution of problem 2 (p2) since the optimal varying beta angle history could assume any value of beta. However, the solution to p1 could introduce large rates for beta gimbal angles which may not be feasible.

Once, the best beta gimbal strategy over an orbit is determined, the average power available over a year can be evaluated by incorporating the motion of the Earth around the Sun, and the nodal regression of the spacecraft orbit. The yearly average available power can also be computed for non-LVLH torque equilibrium attitudes (TEAs). Intra-array shadowing and its resulting power loss can be obtained from PV array geometry and optimal beta tracking solutions and the results compared to shadowing losses for arrays with full sun-tracking.

3. MATHEMATICAL MODEL

The direct sunlight factor P can be written as a function of the orbital elements $\Omega, i, \psi, \gamma, \eta$, the 3-2-1 ordered Euler angles $\hat{\psi}, \hat{\theta}, \hat{\phi}$ representing the station attitude from LVLH, the inner alpha gimbal angle α fixed at 90 degrees (as shown in Figure

1) to minimize drag and the beta gimbal angle control variable β using coordinate transformation matrices. Here, Ω represents the season dependent angle measured from the vernal equinox to the Earth–Sun line in the ecliptic plane and is related to the calendar day of the year by the expression $\Omega = 2 \pi (DOY - 80)/365$. γ is the inclination of the Earth's equator to the ecliptic plane. ψ is the orbit plane ascending node with respect to the vernal equinox and i denotes the orbit inclination with respect to the Earth equator. η represents the true anomaly for the circular orbit.

The coordinate systems (0,1,2) are shown in Figure 2 b [ref. 1]. The LVLH coordinate frame is as shown in Figure 2 a. The body coordinate system (4), the outer articulating truss coordinate system (5) and the PV array coordinate system (6) are as shown in Figure 1. The alpha rotation is along positive y_4 or y_5 axis. The beta rotation is along positive z_5 or z_6 axis. The coordinate transformation matrices from Earth–Sun line coordinate system (0) to LVLH coordinate system (3) are as given below :

$$T_0^1 = \begin{bmatrix} C\gamma C\Omega & S\gamma & -C\gamma S\Omega \\ -S\gamma C\Omega & C\gamma & S\gamma S\Omega \\ S\Omega & 0.0 & C\Omega \end{bmatrix} \quad T_1^2 = \begin{bmatrix} C_i C\psi & -S_i & C_i S\psi \\ S_i C\psi & C_i & S_i S\psi \\ -S\psi & 0.0 & C\psi \end{bmatrix}$$

$$T_2^3 = \begin{bmatrix} C\eta & 0.0 & S\eta \\ 0.0 & 1.0 & 0.0 \\ -S\eta & 0.0 & C\eta \end{bmatrix}$$

T_3^4 is the transformation matrix from LVLH to Body coordinate system (4) given by :

$$T_3^4 = \begin{bmatrix} C\hat{\theta} C\hat{\psi} & C\hat{\theta} S\hat{\psi} & -S\hat{\theta} \\ -C\hat{\phi} S\hat{\psi} + S\hat{\phi} S\hat{\theta} C\hat{\psi} & C\hat{\phi} C\hat{\psi} + S\hat{\phi} S\hat{\theta} S\hat{\psi} & S\hat{\phi} C\hat{\theta} \\ C\hat{\phi} S\hat{\theta} C\hat{\psi} + S\hat{\phi} S\hat{\psi} & C\hat{\phi} S\hat{\theta} S\hat{\psi} - S\hat{\phi} C\hat{\psi} & C\hat{\phi} C\hat{\theta} \end{bmatrix}$$

The transformation matrices from body to array coordinate system (6) are:

$$T_4^5 = \begin{bmatrix} Ca & 0.0 & -Sa \\ 0.0 & 1.0 & 0.0 \\ Sa & 0.0 & Ca \end{bmatrix} \quad T_5^6 = \begin{bmatrix} C\beta & S\beta & 0.0 \\ -S\beta & C\beta & 0.0 \\ 0.0 & 0.0 & 1.0 \end{bmatrix}$$

The unit outward normal vector from the active side of the PV array in array coordinate system (6) is $[1 \ 0 \ 0]^T$, by definition. The Earth-Sun line unit vector $[0 \ 0 \ -1]^T$ can be represented in coordinate frame (6) by pre-multiplying it by transformation matrix T_0^6 . The direct sunlight factor P , which is the dot product of the above unit vectors can now be written as $P = -T_0^6(1, 3)$ during the orbital daylight and $P = 0.0$ during earth occultation. Here, T_0^6 is a 3x3 transformation matrix defined by $T_0^6 = T_5^6 * T_4^5 * T_3^4 * T_2^3 * T_1^2 * T_0^1$. In the initial portion of the study, it is assumed that the vehicle attitude is LVLH and hence the matrix T_3^4 is an identity matrix.

Now the optimal control problem p1 can be defined as follows:

$$\max_{\beta(\eta) \in (PWC[\eta_0, \eta_f])} \int_{\eta_0}^{\eta_f} P(\beta) d\eta$$

where, *PWC* denotes piece-wise continuous functions. One can chose $\eta_0 = 0.0$ and $\eta_f = 2\pi$ without any loss of generality to represent one complete orbit. This is made equivalent to a typical Mayer type optimal control problem [ref. 2] using the the first order ordinary scalar differential equation $\frac{dx}{d\eta} = P(\beta)$ and initial condition $x(t_0) = 0.0$.

The optimal control problem p1 takes the form

$$\begin{aligned} \max \quad & x(\eta_f) \\ \beta(\eta) \in & (PWC[\eta_0, \eta_f]) \end{aligned}$$

subject to the differential equation $\frac{dx}{d\eta} = P(\beta)$ and initial condition $x(t_0) = 0.0$.

Similarly, problem p2 can be written as

$$\begin{aligned} \max \quad & x(\eta_f) \\ \beta(\eta) \in & (\text{constant value } \beta_c \text{ for all } \eta \in [\eta_0, \eta_f]) \end{aligned}$$

subject to the differential equation $\frac{dx}{d\eta} = P(\beta)$ and initial condition $x(t_0) = 0.0$.

4. SOLUTION PROCEDURES

Since optimal control problem p1 does not contain the state x on the right hand side of the differential equation, and since P is always positive semi-definite, the optimal control problem can be simplified to a parameter optimization problem where P has to be maximized at every value of true anomaly during orbital daylight. The functional dependence of P on β is obtained and the best value of β for a given η is obtained by satisfying the conditions

$$\frac{\partial P}{\partial \beta} = 0.0$$

$$\frac{\partial^2 P}{\partial^2 \beta} \leq 0.0$$

For problem p2, a parameter optimization algorithm was used to obtain the optimal beta gimbal angle, which when kept constant over a given orbit maximized the performance index.

The optimal beta can thus be obtained for problem p1 or problem p2 as explained above for a given orbit. For evaluation of performance over an year, a model of the regressing ascending node is used [ref. 3]. The daily rate of change of ψ is as follows :

$$\frac{d\psi}{dt} = \frac{3nC_{20}}{2(1-e^2)} \frac{a_e^2}{a^2} \cos(i)$$

Here n is the orbital rate in radians/sec, and $C_{20} = -.0010827$ is the Earth oblateness coefficient. a_e is the earth radius in meters while a is the orbit radius in meters. e denotes the eccentricity of the orbit and i indicates the orbit inclination as defined earlier. For a nominal altitude of 220 nm and inclination of 28.5 degrees, the rate of change of ascending node can be written as:

$$\frac{d\psi}{dt} = -7.05078 \text{ degrees/day}$$

With this model and suitable initial values of the ascending node, yearly power losses due to optimal beta-tracking strategies can be investigated.

5. NUMERICAL RESULTS (NO SHADOWING CONSIDERATIONS)

a. LVLH Station Core Attitude :

To clearly understand the variation in direct sunlight factor over an orbit, two extreme examples of orbits are used, namely, winter solstice (day 356) with ascending node 180 degrees, and spring equinox (day 80) with ascending node zero as shown in Figure 2 c. The former example has a maximum magnitude of solar beta angle of 52 degrees while the latter example has a minimum magnitude of solar beta angle of zero degrees.

Figure 3a depicts the variation of P over an orbit for winter solstice and ascending node 180 degrees. P has a value of unity for full sun-tracking during the orbital daylight.

The region of occultation due to Earth's shadowing is also depicted. Variation of P for optimal time varying beta angle (solution to p1), variation of P for optimal constant beta angle (solution to p2) and variation of the same with beta angle fixed at the solar beta angle are plotted. The time varying optimal beta angle solution is higher than the other two plots over the entire orbit as expected. The solar beta solution touches unity at one point in the orbit, but has lesser average magnitude than the solution obtained by the optimal constant beta orientation. The percentage power available, defined as the *ratio of the area under the plots of the single-axis beta gimbal strategies to the area under the full sun-tracking graph*, was about 87.4% for optimal time-varying beta, 82.4% for optimal constant beta and 76.9% for beta gimbal angle equalling solar beta.

Figure 3b similarly shows the direct sunlight factor P history for an orbit characterized by a zero ascending node on the day of spring equinox. All the beta-tracking solutions are identically the same for most part of the orbit, except during the entry and exit from the Earth's shadow, where optimal time-varying beta gimbal angle strategy produces a 180 degree flip to obtain sunlight on the active side of the PV array. The percentage power available was about 55.3% for optimal time-varying beta and 53% for optimal constant beta which was same as the solar beta.

It was observed that the average power obtained for problem p1 and the corresponding power for problem p2 were **not** very different for various orbits. The percentage of power improvement by using p1 was in the order of 2–5% over using the constant beta gimbal angle strategy of p2. Figure 4a shows the beta histories for the orbit with ascending node of 180 degrees on winter solstice and Figure 4b depicts the same for the spring equinox, zero ascending node. The large rates (such as 180 degree flip in Figure 4b) introduced by using p1 solutions would not be feasible from an operational, attitude control, or structural dynamics point of view. Hence, in the forthcoming sections of the paper, only the optimal constant beta gimbal strategy is used.

With the ascending nodal regression model as given earlier and with optimal constant beta gimbal tracking, a simulation was performed for one complete year with the initial ascending node assumed to be zero degrees at day zero. The ratio of the the available power using the optimal constant (implies constant over an orbit, but slowly changes from orbit to orbit) beta strategy to the power available using full sun-tracking is depicted in Figure 5. The yearly average power available is about 60% of full sun-tracking power. The

yearly average power was re-computed for various initial conditions of the ascending node. However, the variation in average power was minimal and hence it can be tacitly assumed that the average available power is independent of the initial ascending node. The actual power available may be more due to reduced shunt losses when compared to full sun-tracking. The yearly variation of the optimal beta angle is compared to the solar beta angle in Figure 6, for an initial ascending node of zero degrees. The magnitude of the optimal beta angle is **always** greater or equal to the magnitude of the solar beta angle. This result has some special implication in intra-array shadowing, which is discussed in a later section.

b. Non-LVLH Station Attitude :

The steady state attitude of the core of the Space Station does not remain at LVLH, but oscillates about the Torque Equilibrium Attitude (TEA). The TEA is a function of the Space Station configuration, the operating altitudes and atmospheric disturbance torques. It is desired that the TEAs be within a ± 5 degrees about the LVLH, for payload pointing requirements. However, for earlier flight configurations, large pitch TEAs are possible [ref. 4]. In this study, conservative maximum variations in the attitude of ± 10 degrees for roll and yaw and ± 20 degrees for pitch are assumed. The only change in the analysis from the previous section is the value of the elements in matrix T_3^4 . Yearly power availability (% of full sun-tracking power) is obtained as before for different TEAs in this range and the values are plotted in Figure 7. The variations in power availability are less than 2% for this range of attitude deviations from local vertical.

6. NUMERICAL RESULTS WITH INTRA-ARRAY SHADOWING

The analysis performed above assumes that the PV arrays do not shadow each other at any time. However, the validity of this assumption depends upon the geometry of the arrays, namely, the width ($2a$) of the arrays and the distance (b) between the parallel beta axes and the solar geometry which is a function of the beta gimbal angle β and the solar beta angle β_s , as shown in Figure 8. The geometry shows the sun rays on the plane of the

paper which is a worst case shadowing phenomenon for the beta-only tracking problem (Figure 8 is always true for full sun-tracking arrays).

The model of the Space Station used, as shown in Figure 1, has the inner PV arrays separated by 77 feet ($b = 23.47$ m). The width of each array is 38.9 feet ($2a = 11.857$ m). The port and starboard outer solar arrays are separated from the adjacent inner arrays by 44 feet ($b = 13.41$ m). Figure 8 can be used to prove that for shadowing to occur the following equation must be satisfied;

$$\frac{\sin\beta}{\tan(\frac{\pi}{2} - \beta_s)} + \cos\beta \geq \frac{b}{2a}$$

Since the inner array separations are larger than the separation between the adjacent port or starboard arrays, the latter plays the dominant role in causing shadowing. Figure 9 shows the variation of the left hand side of the above equation defined as the **shadowing function** with β for various values of β_s . The right hand side of the above equation is a constant (equal to 1.13117 for the two adjacent inner and outer PV arrays) for a given configuration geometry. Figure 9 clearly shows that for a given β_s , the shadowing function peaks at $\beta = \beta_s$. Shadowing may occur only if the shadowing function curve crosses the $b/2a$ line as shown in Figure 9. The smallest value of β_s at which the shadowing function crosses this line for **any** β is at $\beta_s = 27.86$ degrees. In other words, no shadowing occurs for **any** beta angle if the solar beta angle is less than 27.86 degrees. For solar beta angles greater than this value, the shadowing function cuts the $b/2a$ line at two points. For a given solar beta angle, if the beta gimbal angle is such that the corresponding shadowing function value is greater than $b/2a$, then partial shadowing between arrays will occur over some portion of the orbit.

Figure 10 shows the typical variation in sun-tracking beta angle and constant optimal beta angle with the solar beta angle (this is obtained from part of the data in Figure 6) for an LVLH attitude. A shadowing threshold line is also plotted in the same figure. The shadow region is obtained from the beta gimbal angle at the intersection points of the shadowing function with the $b/2a$ line of Figure 9. The region of partial shadowing during por-

tions of each orbit is shaded in Figure 10. If the optimal beta angle strategy is used, shadowing occurs only for beta gimbal angles greater than the critical value of 35 degrees, which corresponds to the intersection of the optimal constant beta line with the shadowing threshold line. For full sun-tracking strategy, the beta gimbal angle is same as the solar beta (for LVLH attitudes) and hence shadowing will occur at angles greater than 27.86 degrees. Prior to deployment of the outer PV arrays, no shadowing can ever occur, since the critical value corresponding to the larger $b/2a$ is greater than the maximum possible solar beta angle of 52 degrees.

The ratio of the the available power using the optimal constant beta strategy to the power available using full sun-tracking has been shown in Figure 5. A similar graph with shadowing considerations is shown in Figure 11. The regions of *occasional* partial shadowing using optimal beta tracking and the regions of *continuous* partial shadowing for full sun-tracking are shown. The former is obtained by shading the time regions in the beta-tracking plot, where the solar beta is greater than the critical value of 35 degrees. The latter is obtained by shading the time regions in the full sun-tracking plot, where the solar beta angle is greater than 27.86 degrees.

The results indicate that, for the particular configuration studied, days of occasional shadowing constitute about 18% of the year for optimal beta tracking. Exact power loss due to shadowing can be obtained by more sophisticated ray-tracing methods, etc.. Days of continuous partial shadowing constitute about 30% of the year for full sun-tracking. Hence the actual ratio of available power for such configurations (which have shadowing problems) using optimal beta-tracking may be better than the nominal value of approximately 60% as obtained in section 5 without shadowing considerations.

7. A COMPARISON TO OPTIMAL ALPHA-ONLY TRACKING

For alpha-tracking only, the alpha joints are free to rotate, and it is assumed that the beta angles are fixed at zero (as shown in Figure 1). The optimal alpha angle history to be determined, over a given orbit is that which maximizes the available power, assuming LVLH attitude. Occultation effects are also taken into consideration. The analysis is exactly the same as for problem p1, except the fact that the angle $\alpha(\eta)$ is the control variable and $\beta = (0,0)$ is the constant beta gimbal angle. The zero beta angle is chosen since the solar

beta angle (which is used for full sun-tracking beta gimbal angle) varies from + 52 degrees to -52 degrees. The Mayer problem as detailed earlier is constructed and the optimal control histories for alpha gimbal angle are obtained.

Figure 12 shows the optimal alpha joint gimbal histories over one orbit for a best case of spring equinox with zero ascending node (zero solar beta angle) and a worst case of winter solstice with 180 degrees ascending node (maximum solar beta angle of 52 degrees). The alpha history is linear, varying by 360 degrees per orbit. Figure 13 shows the variation of the direct sunlight factor over the two orbit cases described above. The direct sunlight factor is a constant over an orbit due to the fact that the normal to the orbit plane and the alpha gimbal axis are parallel. The direct sunlight factor is equal to the cosine of the solar beta angle corresponding to the particular orbit. Thus for the best case orbit, 100% of the full sun-tracking power is obtained. For the worst case orbit, only 61.57% of the full sun-tracking power is available.

As performed in the beta-only tracking strategy, the model of the regression of ascending node is used to evaluate the average available power over one year. Figure 14 gives the yearly variation of the ratio of power available from optimal alpha-only tracking to full sun-tracking power. This graph would be exactly the same as the variation of the cosine of the solar beta angle over a year. The yearly average power available is approximately 90% of the full sun-tracking power. This value is relatively independent of the initial ascending node magnitude.

Finally, the change in the yearly average power with variations in vehicle attitude is studied. Worst case plausible TEAs are chosen with variations in attitude of ± 10 degrees for roll and yaw and ± 20 degrees for pitch. Figure 15 plots the available power (%) for these non-LVLH attitudes. The variations are minimal.

It should be noted that the alpha-only tracking solutions with $\beta = 0.0$ avoids any intra-array shadowing! If the Space Station configuration design has array geometry which causes shadowing for full sun-tracking, then the actual power loss by using alpha-only tracking may be even less than the average inferred value of 10%!

8. CONCLUSIONS

a. Optimal Beta-tracking strategy :

Assuming a 28.5 degrees inclination and LVLH attitude, optimal constant (constant over an orbit) beta gimbal strategy produces an average of only 60% of the full sun-tracking power over a year. On any given day the reduction may be as low as 17% or as high as 49% of the full sun-tracking power. Using an optimal time-varying beta gimbal angle improves the power availability by a *small* amount (about 2-5%). However, this may require large beta angle rotation rates over an orbit. "Power reduction" has been used synonymous with "sun-light reduction". However, in reality, shunt losses are likely to be reduced for the optimal beta tracking when compared to full sun-tracking.

For an LVLH attitude, an additional bonus for the optimal beta tracking strategy, is that the arrays are oriented edge-on (feathered) with respect to the velocity vector. This minimizes drag, increases orbital lifetime and decreases atomic oxygen degradation effects.

For variations in attitude of ± 10 degrees in roll and yaw and/or ± 20 degrees in pitch, less than 2% additional power loss occurs.

For the configuration studied, prior to deployment of the outer solar arrays, no shadowing between the inner port and starboard arrays were found. Subsequent to deployment of the outer solar arrays, occasional partial shadowing between adjacent arrays occurs for solar beta angles greater than 35 degrees. This constitutes about 65 days (18%) in an year. The shadowing only occurs for a few minutes in an orbit. For the same configuration, with full sun-tracking, continuous (through out the sun-lit portion of the orbit) partial shadowing occurs for solar beta angles greater than 27.86 degrees. This constitutes about 110 days (30%) in an year.

b. Optimal Alpha-tracking strategy :

Assuming a 28.5 degrees inclination and LVLH attitude, optimal alpha gimbal strategy produces an average of 90% of the full sun-tracking power over a year. On any given day the power availability may be as low as 62% or as high as 100% of the full sun-tracking power.

For variations in attitude of ± 10 degrees in roll and yaw and/or ± 20 degrees in pitch, up to an additional 1.5% power loss can occur.

No power loss due to shadowing occurs for this strategy if the beta angle is kept constant at zero.

9. REFERENCES

1. Heck, M.L., "Rigid Body Control Dynamics, Part II", *AMA Report No. 83-22*, NASA purchase order # L-56210B, October 1983, pp. 19-22.
2. Ewing, G.M., "Necessary Conditions for an Extremum", *Calculus of Variations*, Dover Publications, N.Y., 1969.
3. Kaula, W.M., "Theory of Satellite Geodesy", Blaisdell Publishing Company.
4. Kumar, R.R., Heck, M.L., and Robertson, B.P., "Predicted Torque Equilibrium Attitude Utilization for Space Station Attitude Control", *AIAA paper no. 90-3318, AIAA GN&C Conference*, Portland, Oregon, August 20-22, 1990.

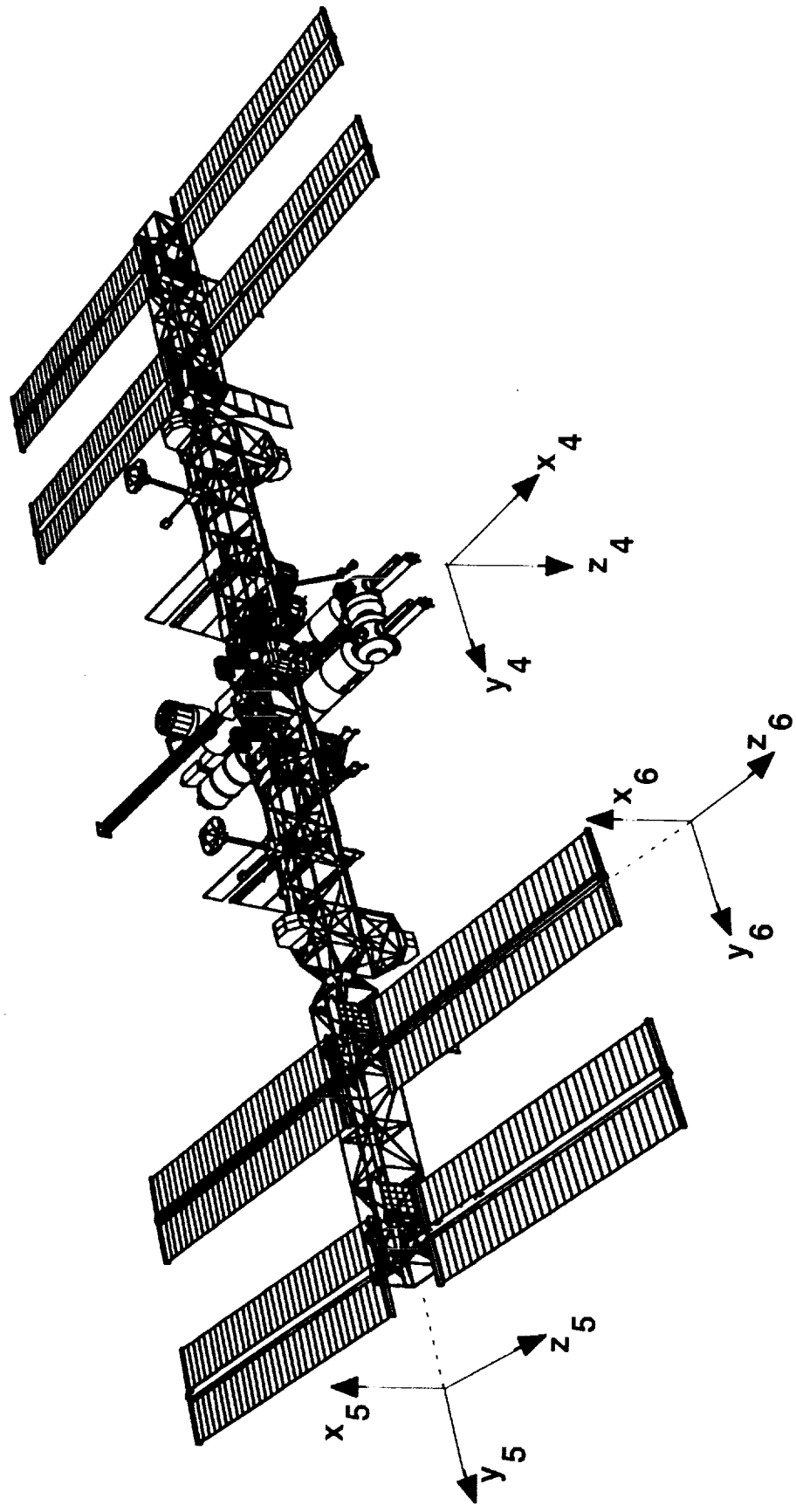


Figure 1 : Space Station Assembly Complete Configuration

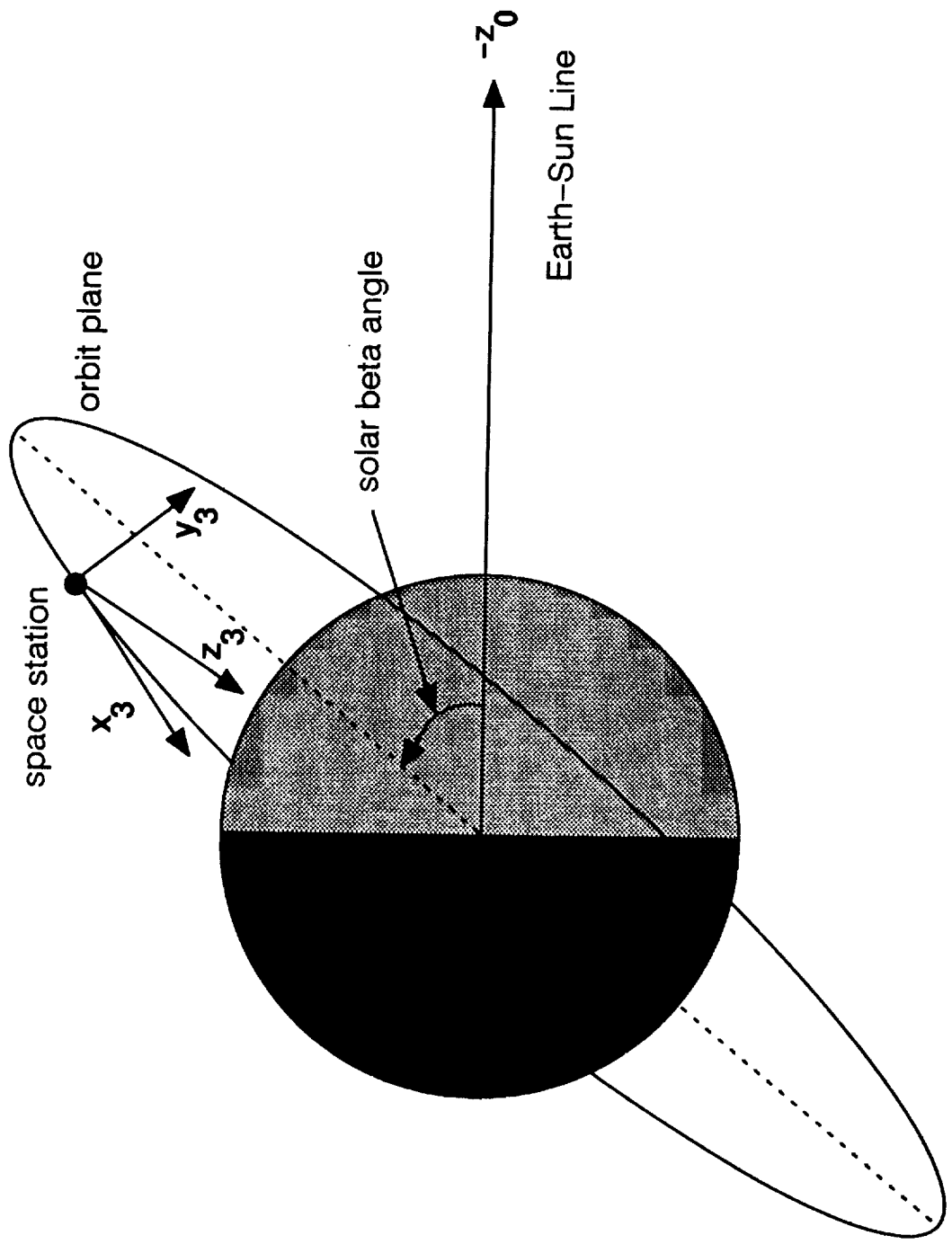


Figure 2 a : Definition of Solar Beta Angle

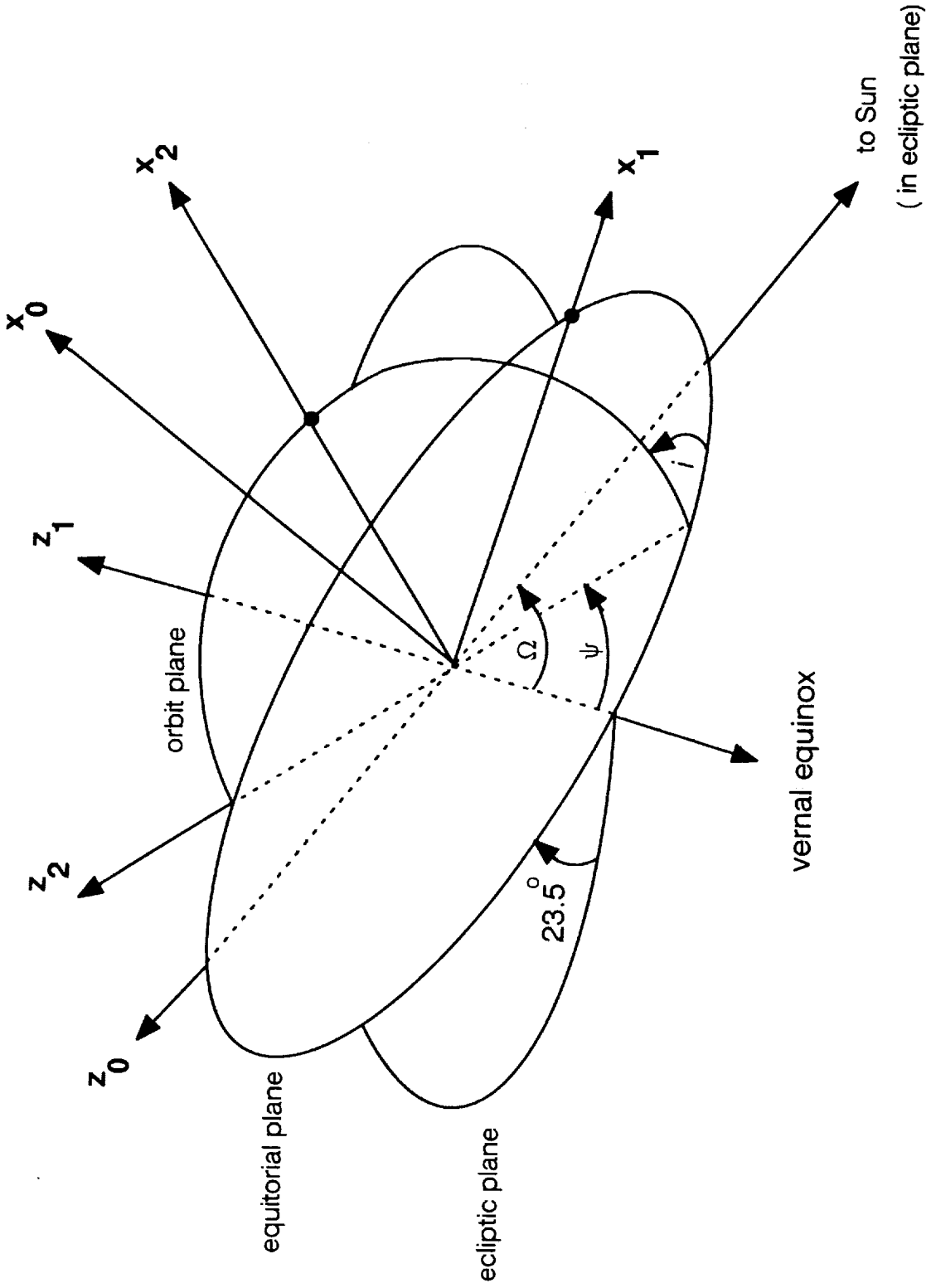


Figure 2 b : Definition of Intermediate Coordinate Systems

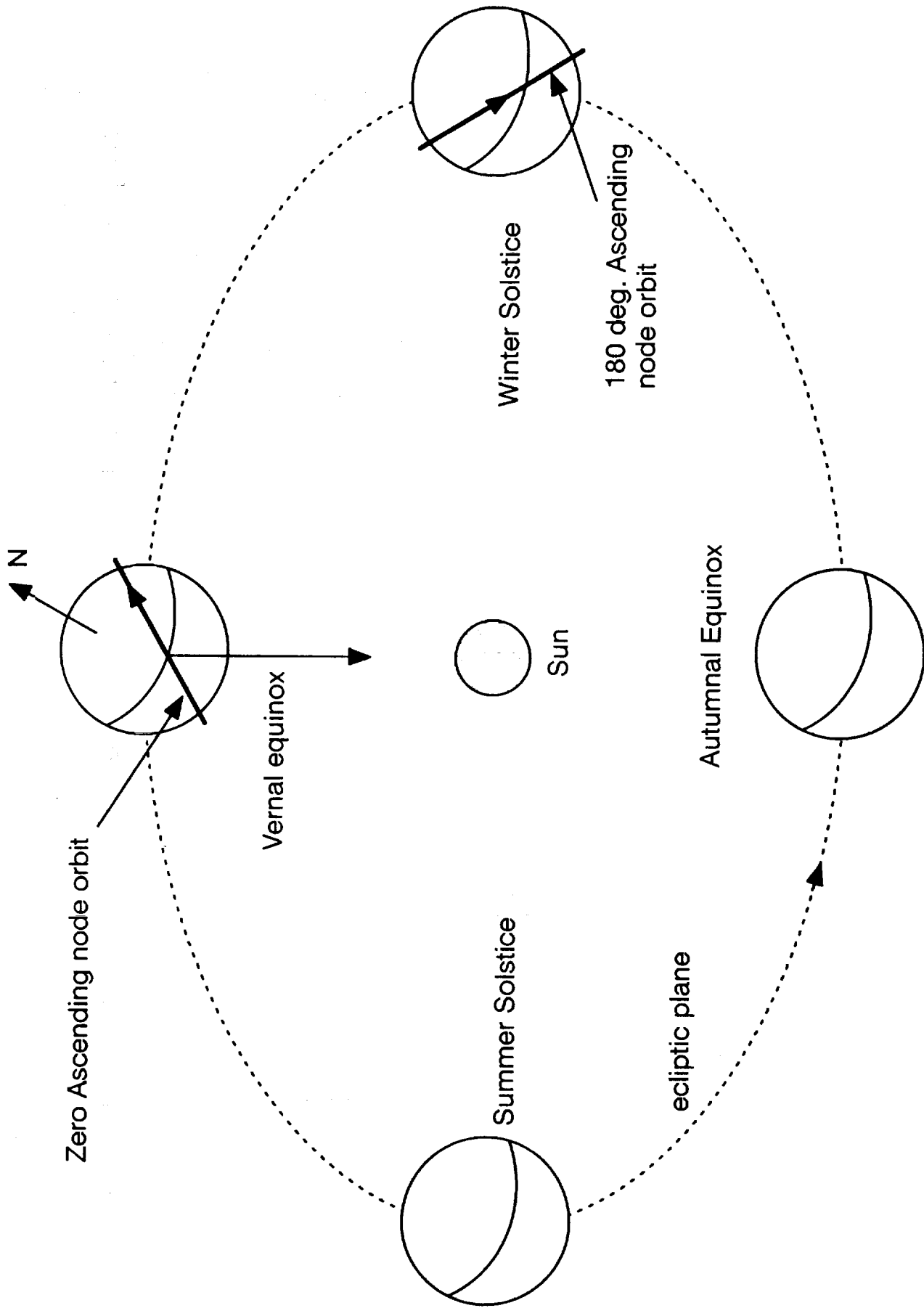


Figure 2 c : Definition of Best and Worst Case Orbits

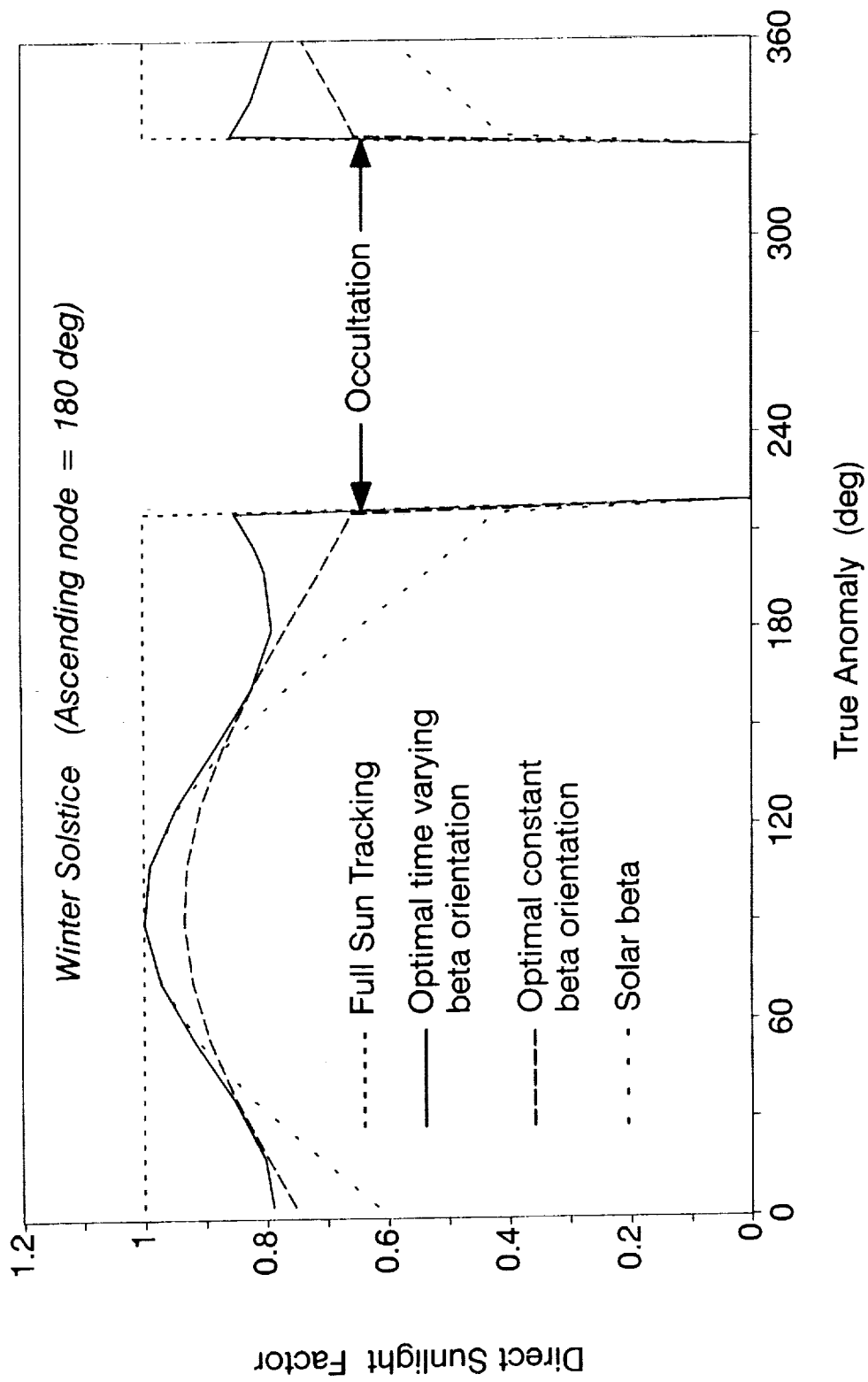


Figure 3a : Variation of Direct Sunlight Factor over a Best Case Orbit

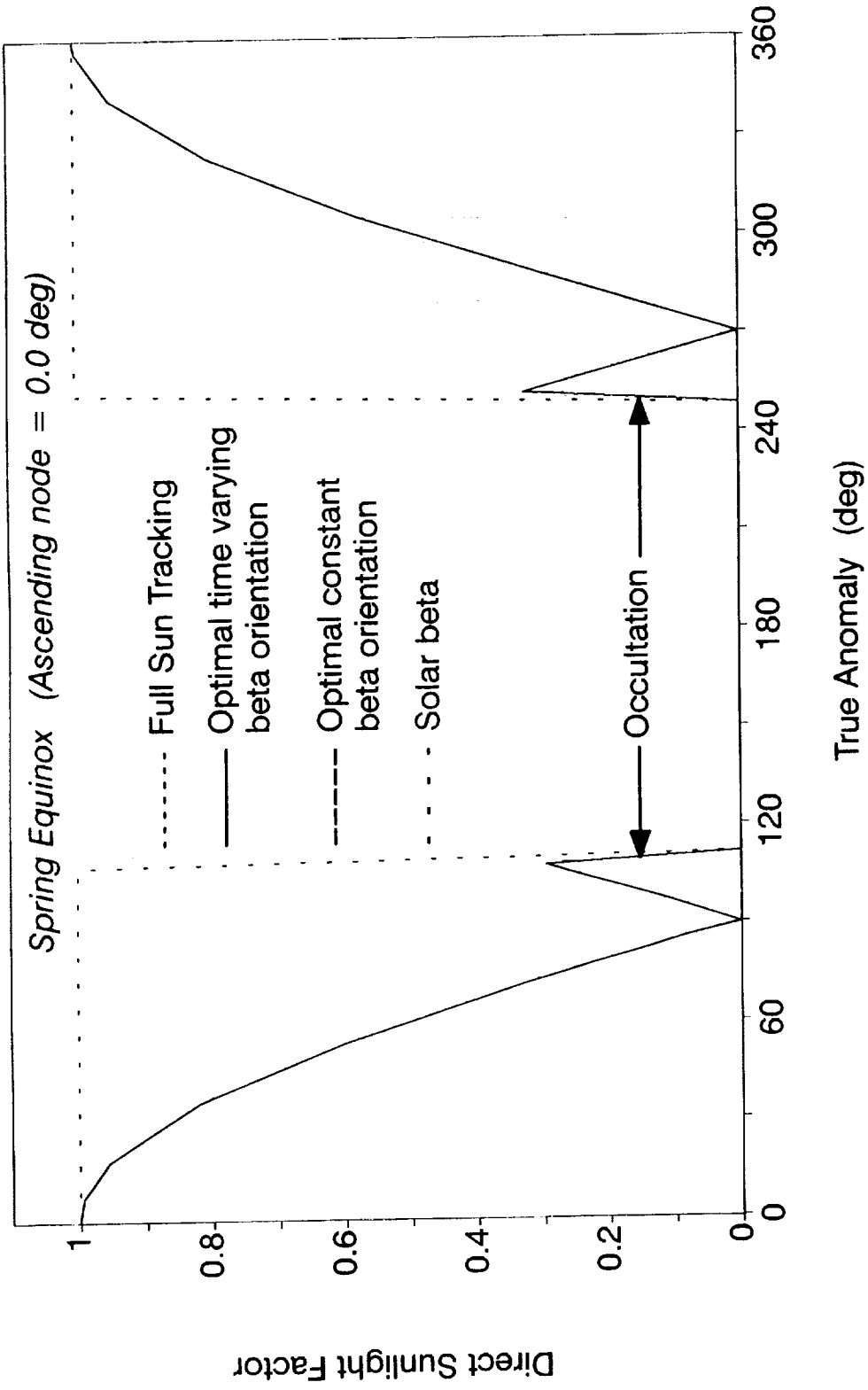


Figure 3b : Variation of Direct Sunlight Factor over a Worst Case Orbit

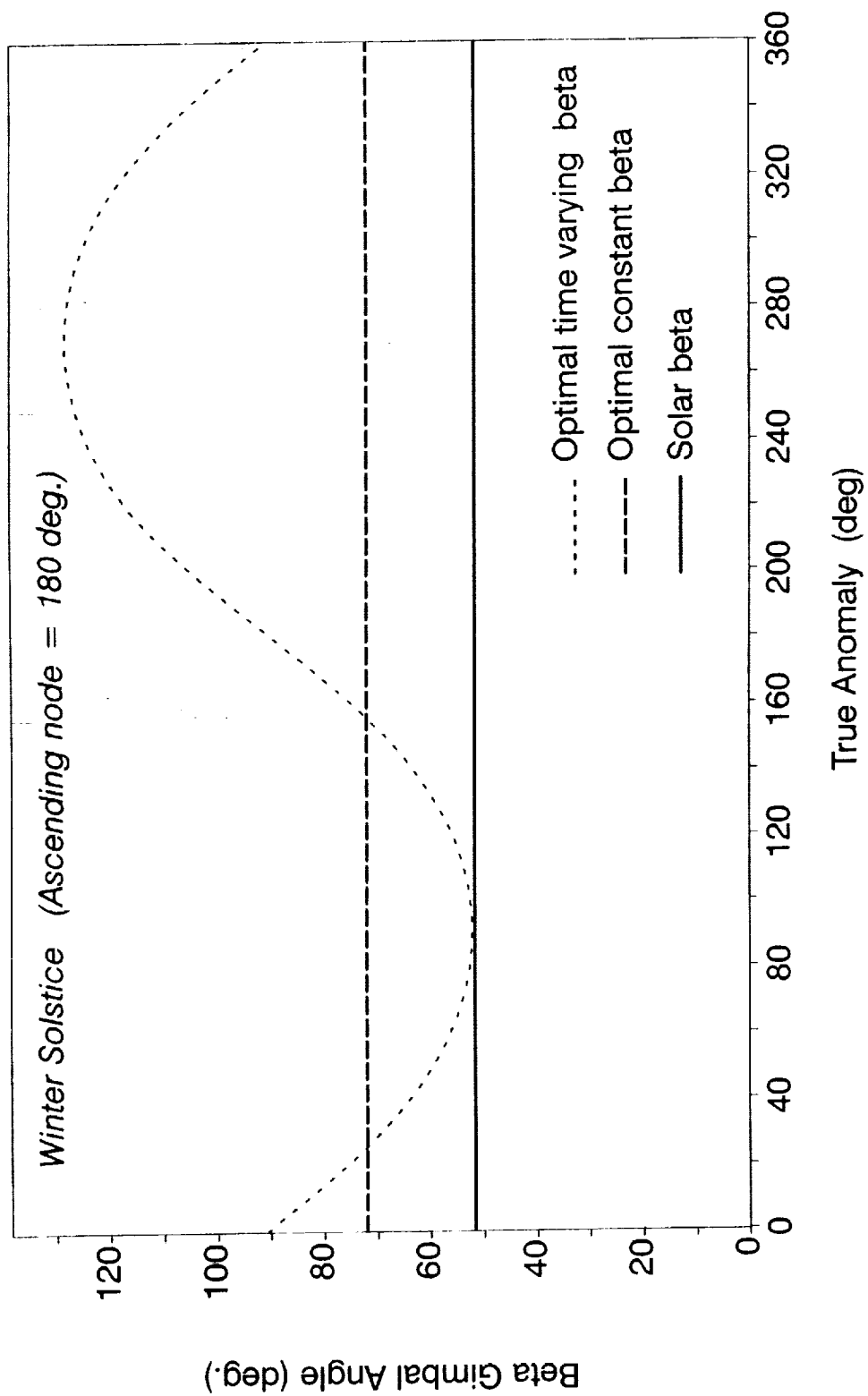


Figure 4a : Beta Gimbal Histories over a Best Case Orbit

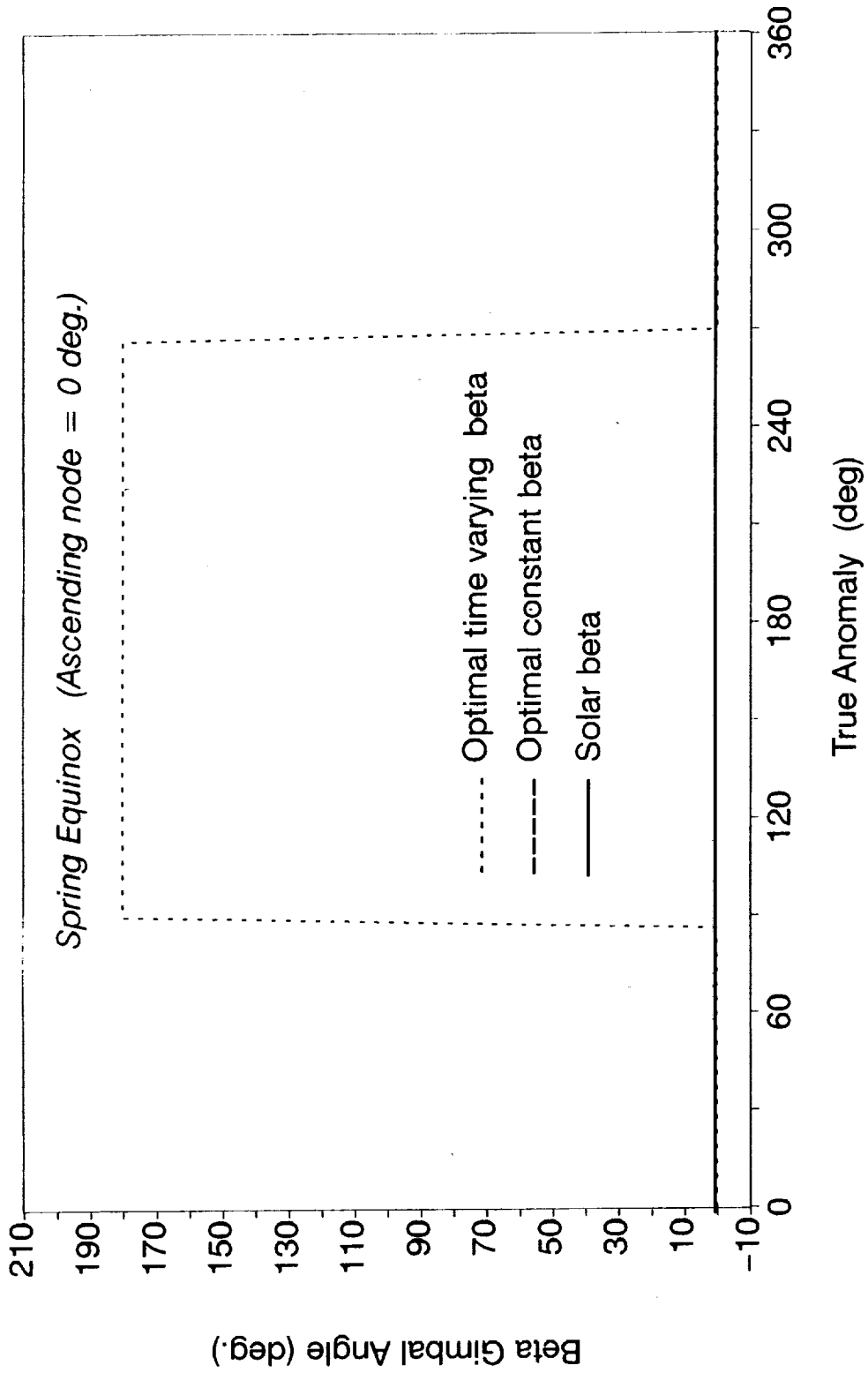


Figure 4b : Beta Gimbal Histories over a Worst Case Orbit

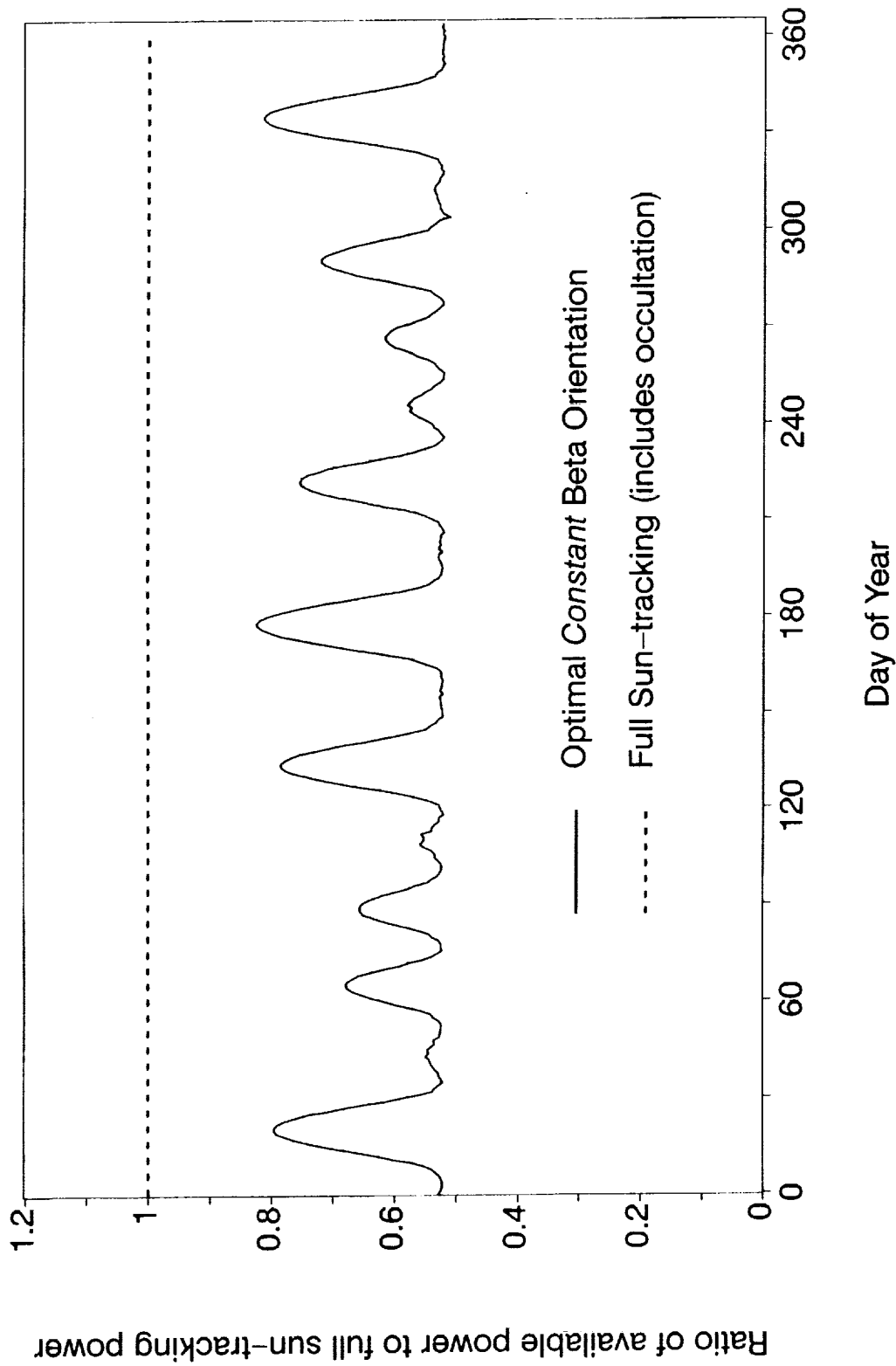


Figure 5 : Yearly Power Availability with Optimal Constant Beta Gimbal Rotation

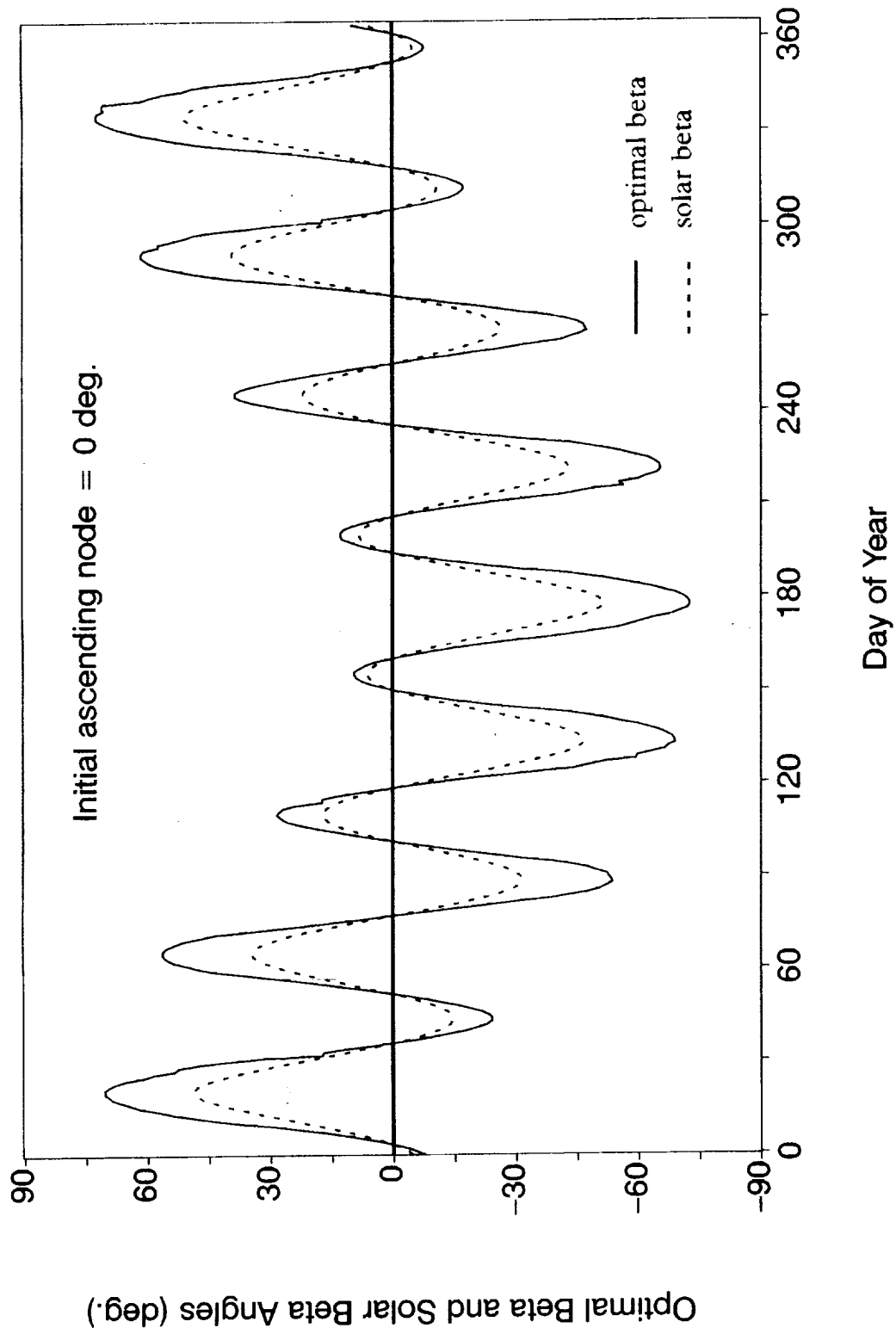


Figure 6 : Yearly Variation of Optimal Constant Beta and Solar Beta

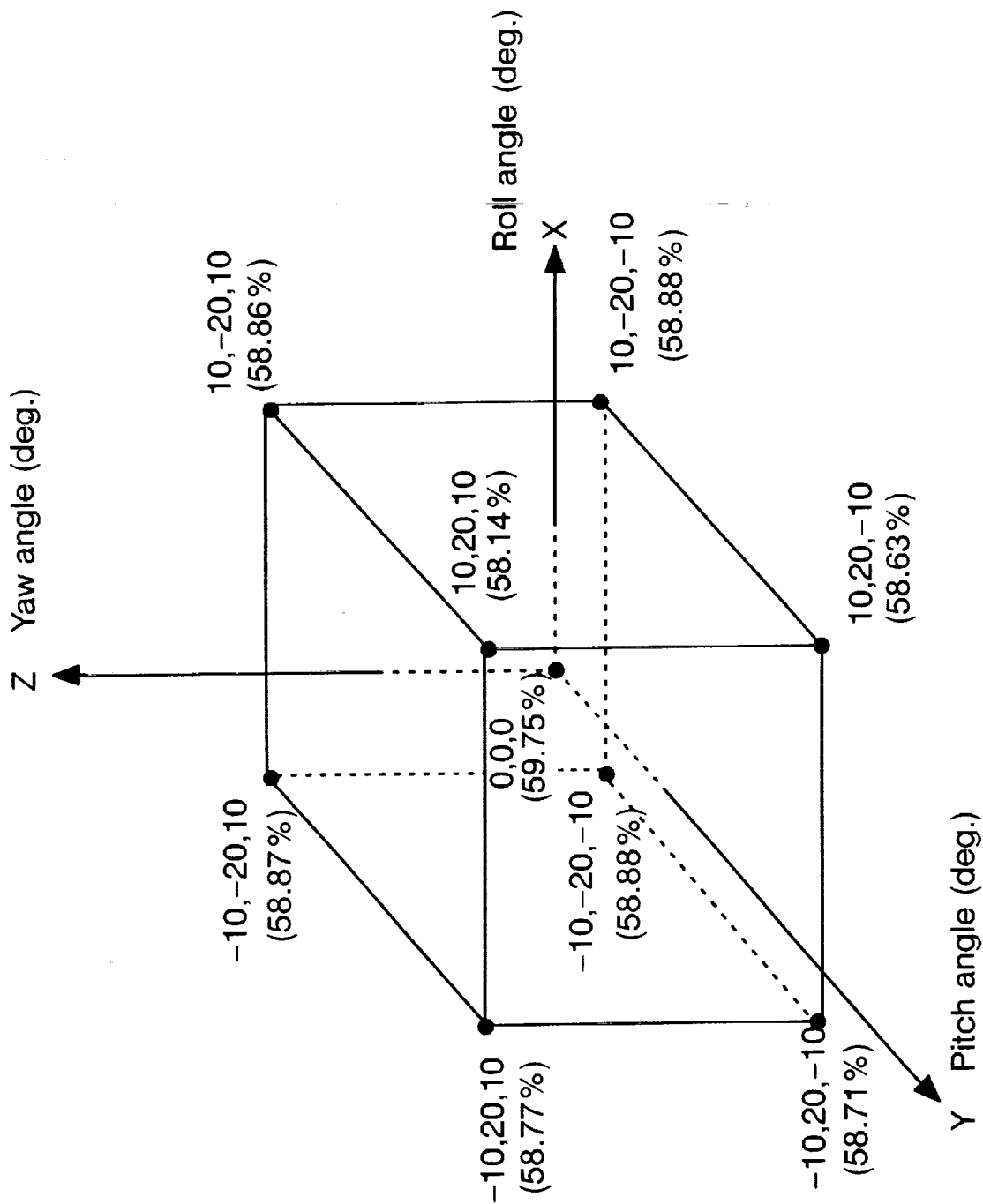


Figure 7 : Yearly Power Availability with Optimal Beta Tracking for Non-LVLH Attitude

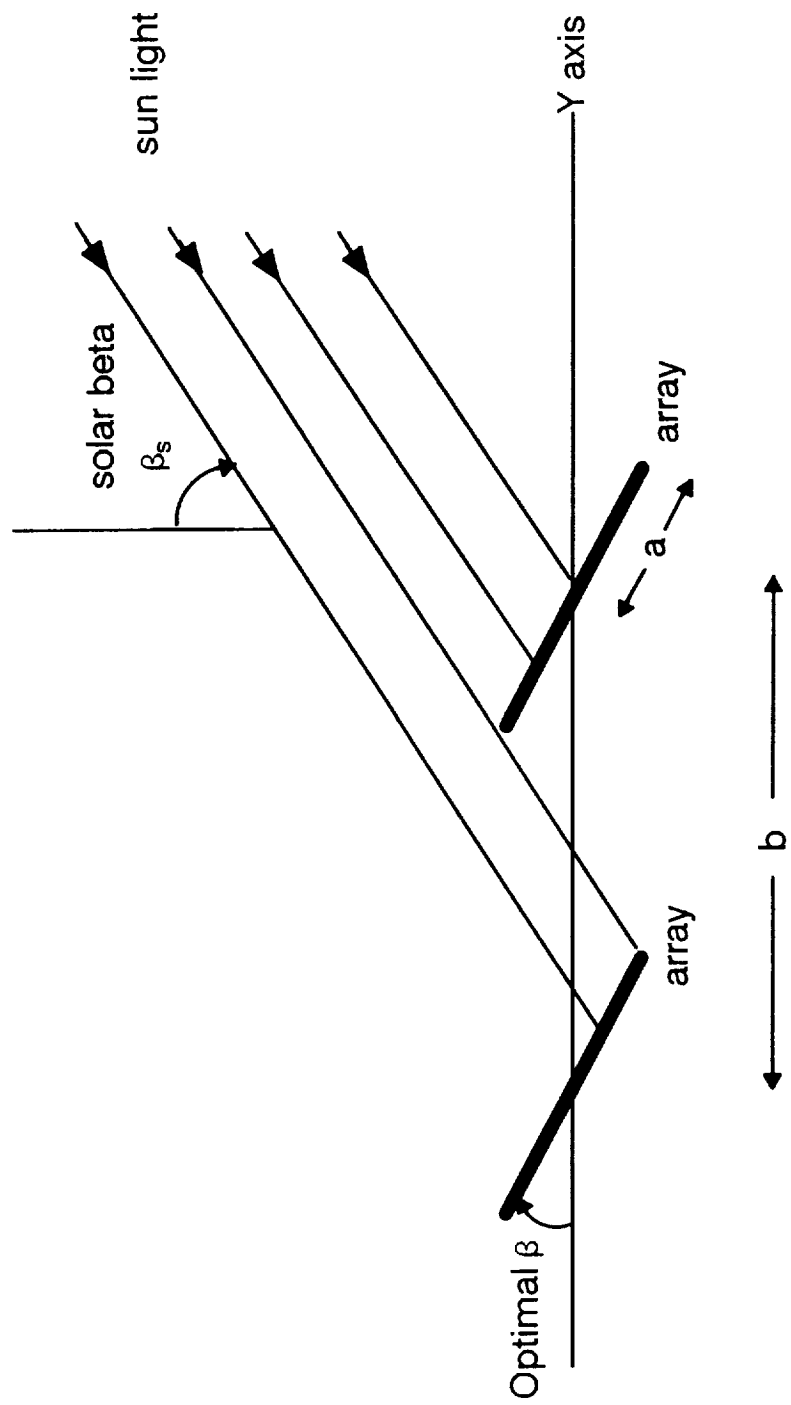


Figure 8 : Array Shadowing Geometry

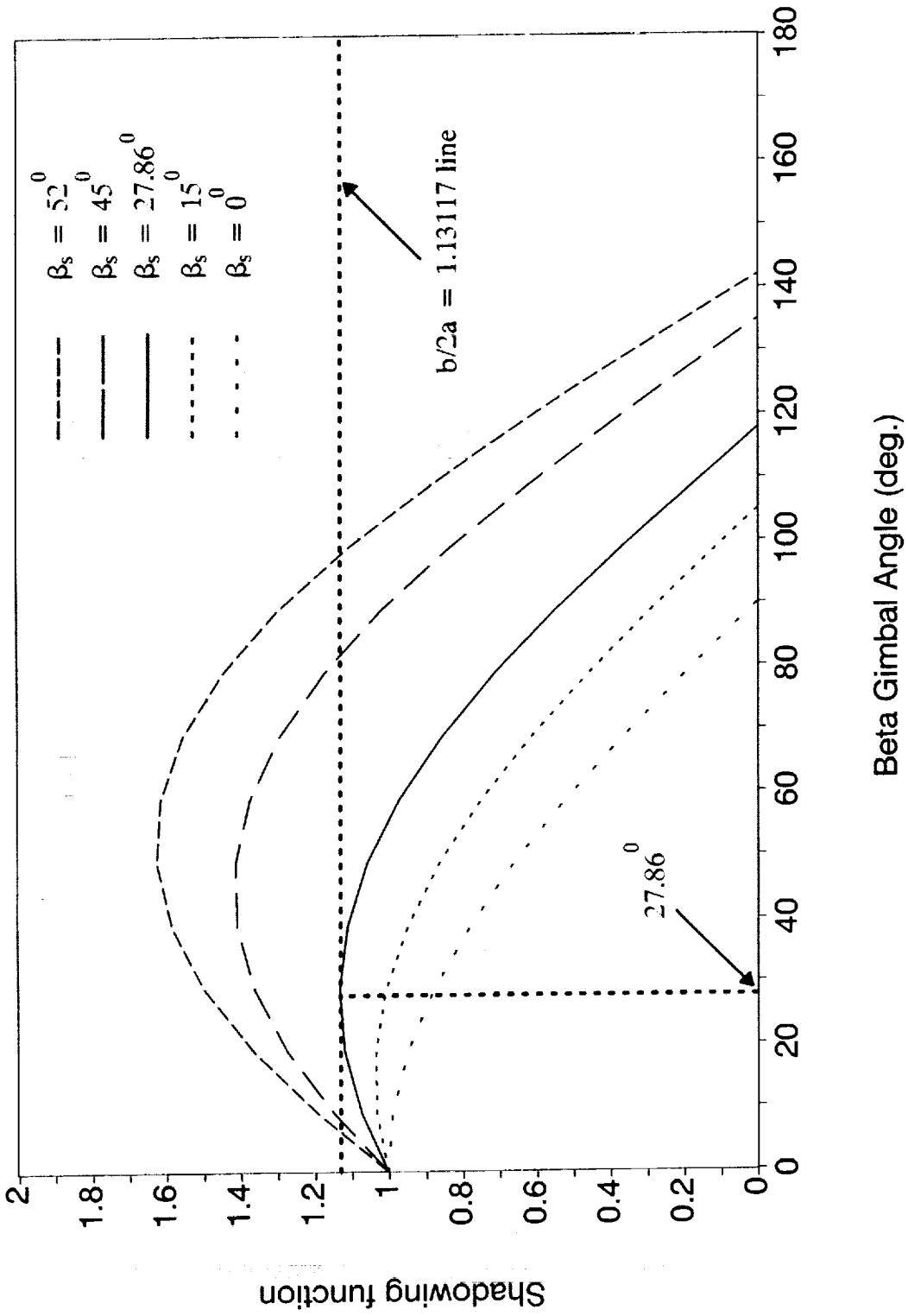


Figure 9 : Variation of Shadowing Function with Beta Gimbal Angle

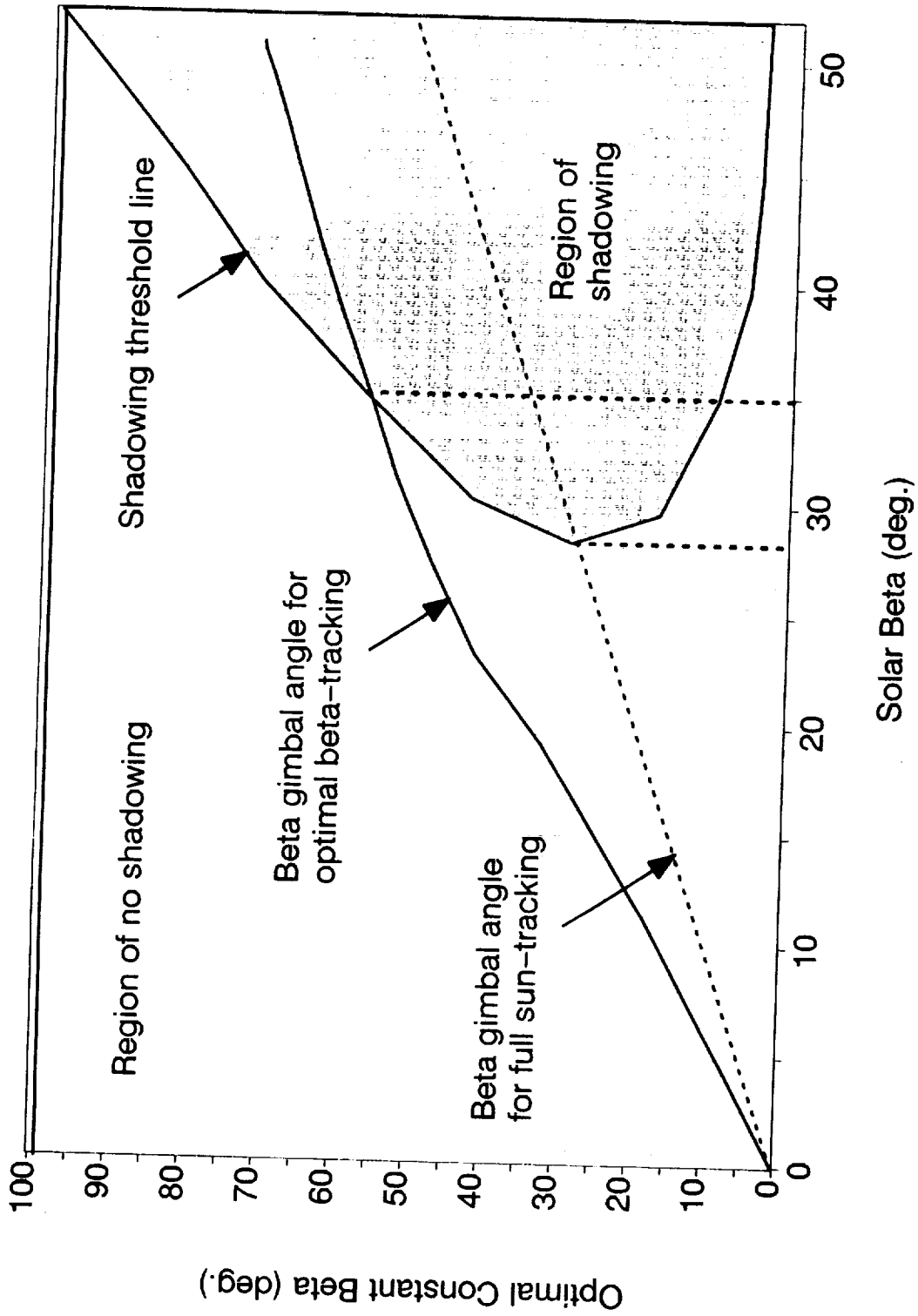


Figure 10 : Beta Gimbal Regions of Solar Array Shadowing

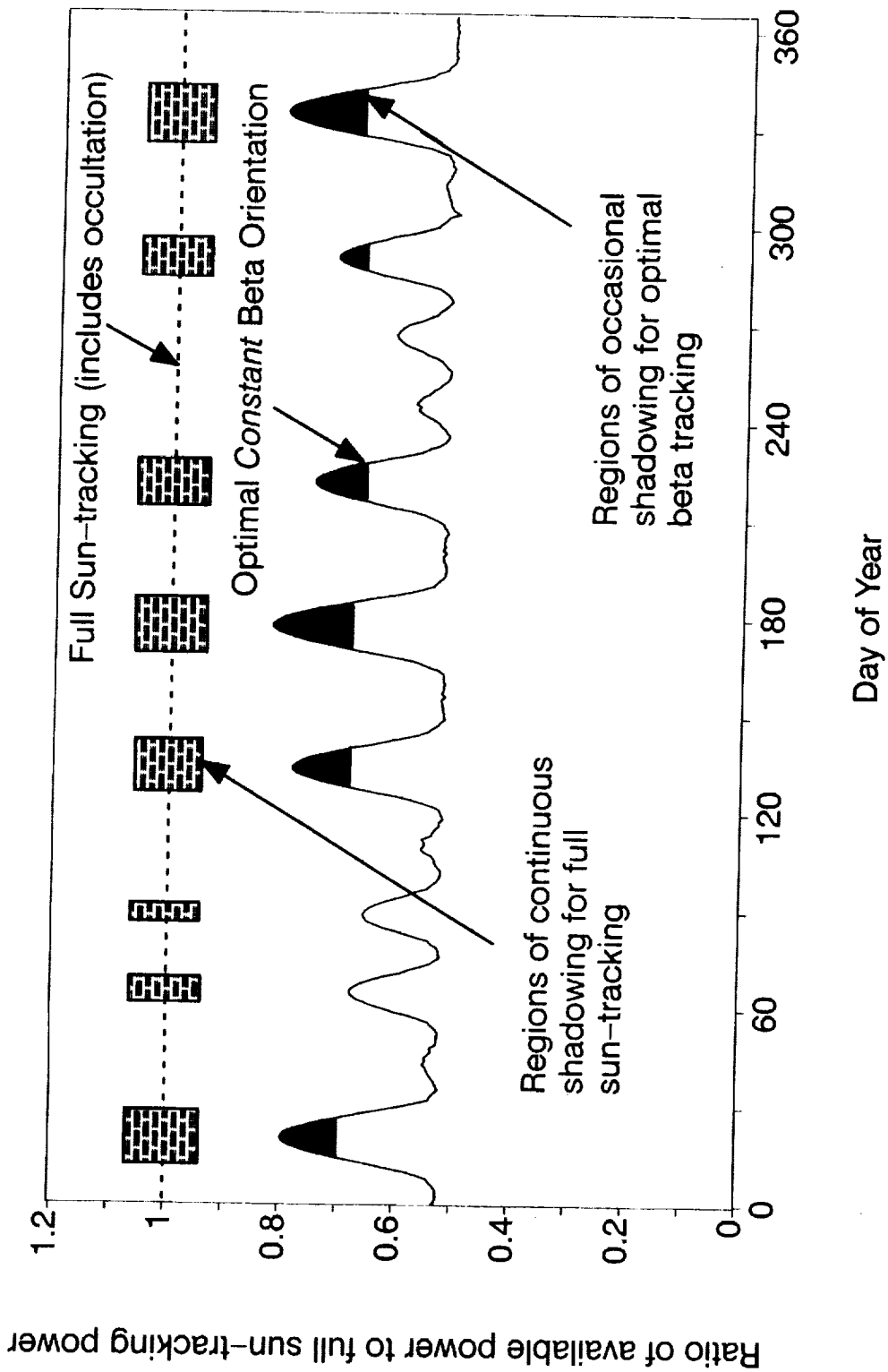


Figure 11 : Yearly Power Availability with Regions of Occasional Shadowing

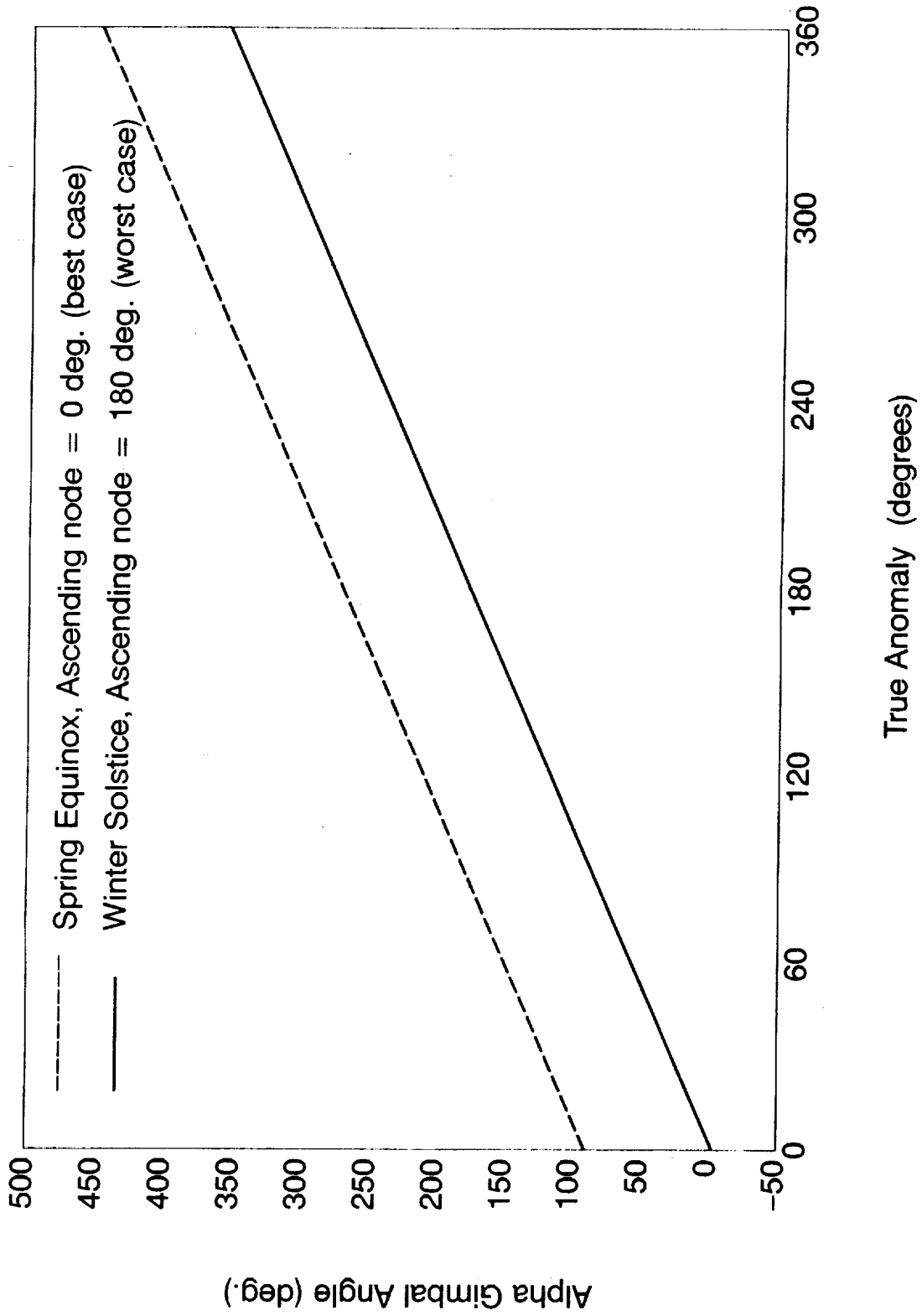


Figure 12 : Optimal Alpha History over Best and Worst Case Orbits

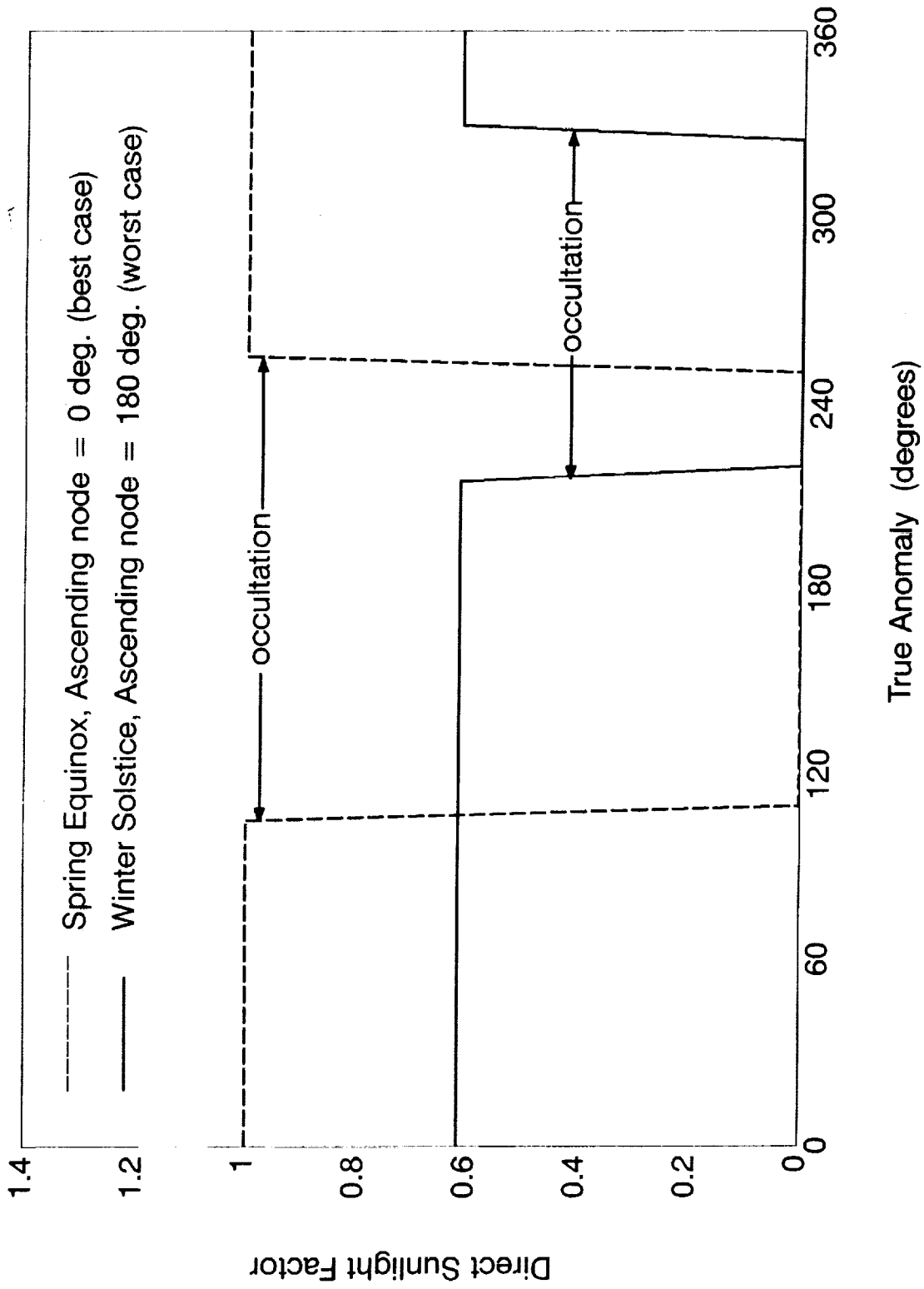


Figure 13 : Variation of Direct Sunlight Factor over Best and Worst Case Orbits with Optimal Alpha Tracking

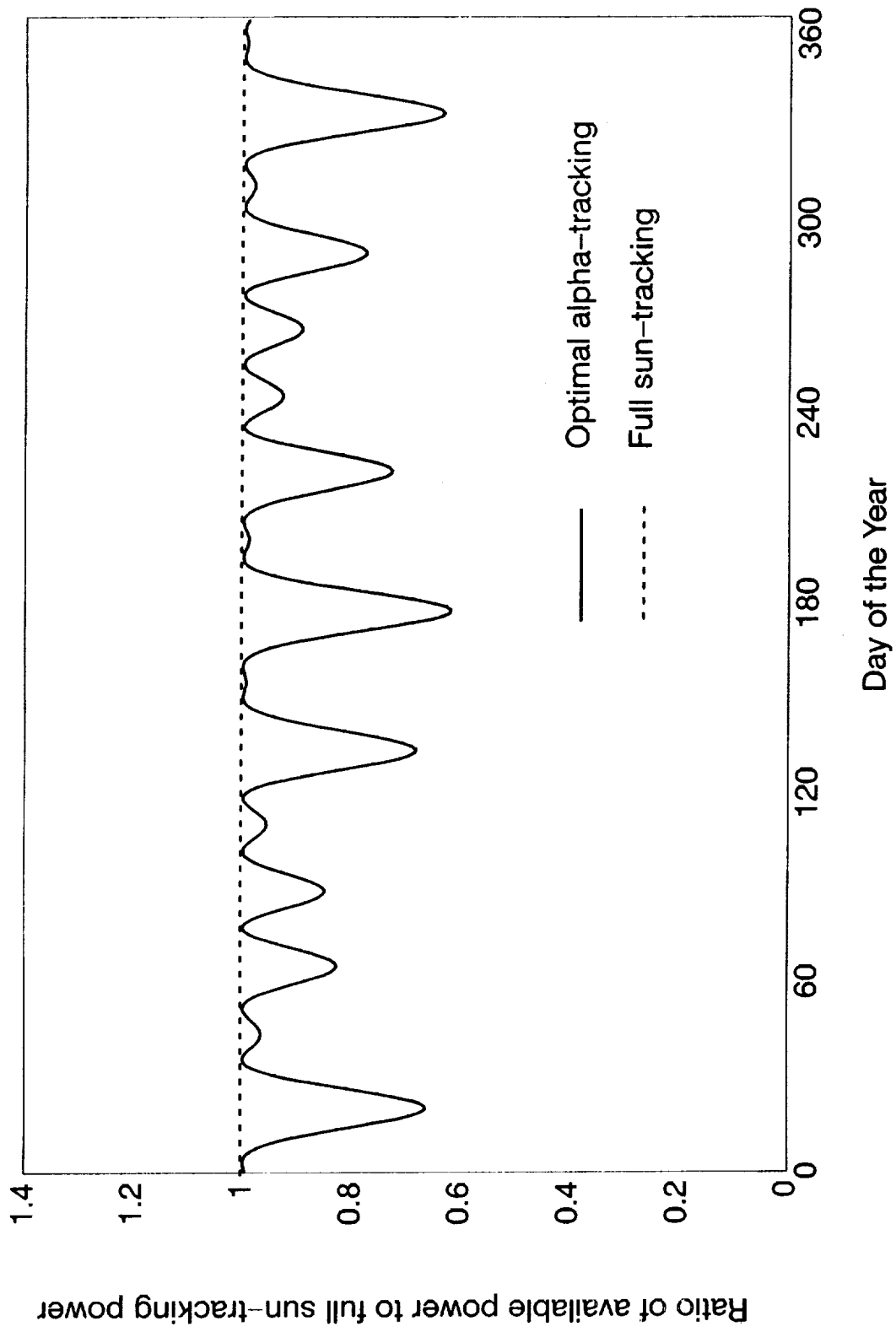


Figure 14 : Yearly Power Variation with Optimal Alpha-Tracking

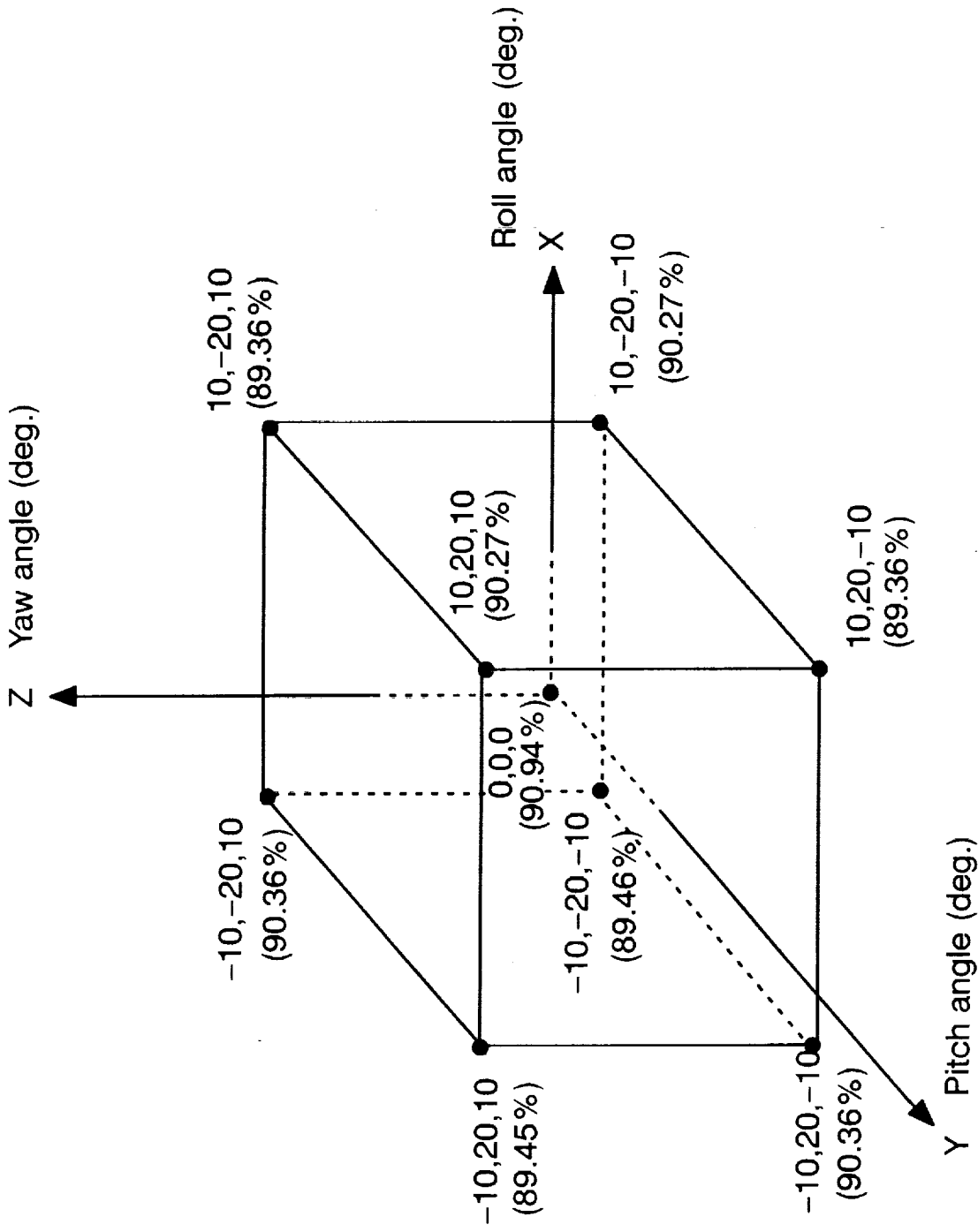


Figure 15 : Yearly Power Availability with Optimal Alpha Tracking for Non-LVLH Attitude

Acknowledgments

The authors would like to acknowledge the guidance and direction offered by LaRC Space Station Office Manager Joe Talbot, and the SSFO Systems Engineering and Analysis Office Manager Richard Russell. This work was performed under NASA contract NAS1-18935.



Report Documentation Page

1. Report No. NASA CR-187510	2. Government Accession No.	3. Recipient's Catalog No.	
4. Title and Subtitle Power Optimal Single-axis Articulating Strategies	5. Report Date February 1991	6. Performing Organization Code	
	7. Author(s) R. R. Kumar and M. L. Heck	8. Performing Organization Report No. 91-1	
9. Performing Organization Name and Address Analytical Mechanics Associates, Inc. 3217 N. Armistead Avenue, Suite G Hampton, VA 23666	10. Work Unit No. 476-14-15-01	11. Contract or Grant No. NAS1-18935	
	12. Sponsoring Agency Name and Address National Aeronautics and Space Administration Langley Research Center Hampton, VA 23665-5225	13. Type of Report and Period Covered Contractor Report	14. Sponsoring Agency Code
15. Supplementary Notes Langley Technical Monitor: Richard A. Russell Task 1			
16. Abstract Power optimal single-axis articulating PV array motion for Space Station Freedom is investigated. The motivation is to eliminate one of the articular joints to reduce Station costs. Optimal (maximum power) Beta-tracking is addressed for LVLH and non-LVLH attitudes. Effects of intra-array shadowing are also presented. Maximum power availability while Beta-tracking is compared to full sun-tracking and optimal alpha-tracking. The results are quantified in orbital and yearly minimum, maximum and average values of power availability.			
17. Key Words (Suggested by Author(s)) Optimal Single-axis Tracking, Solar Beta Angle, Shadowing	18. Distribution Statement Unclassified - Unlimited Subject Category 39		
19. Security Classif. (of this report) Unclassified	20. Security Classif. (of this page) Unclassified	21. No. of pages 36	22. Price A03